OMTM, Volume *26*

Supplemental information

Targeted biallelic integration of an inducible Caspase 9 suicide gene in iPSCs for safer therapies

Stephanie Wunderlich, Alexandra Haase, Sylvia Merkert, Kirsten Jahn, Maximillian Deest, Helge Frieling, Silke Glage, Wilhelm Korte, Andreas Martens, Andreas Kirschning, Andre Zeug, Evgeni Ponimaskin, Gudrun Göhring, Mania Ackermann, Nico Lachmann, Thomas Moritz, Robert Zweigerdt, and Ulrich Martin

Supplement

Supplementary Tables

Table S1: Primers and expected sizes of PCR products. Please see figure S1 for schematic illustration of the primer positions. Abbreviations: IT, Integrated transgene; RAS, Reverse antisense; WT, Wild type.

	Forward primer	**RAS primer**	**Product size**
5‘junction	Forward CCA GCT CCC ATA GCT CAG TCT G	RAS ATG GGG AGA GTG AAG CAG AA	1535bp
3‘junction	Forward CCC CTG CTG TCC ATT CCT TA	RAS GTG AGT TTG CCA AGC AGT CA	1503bp
homo-vs. heterozygous	Forward CCA GCT CCC ATA GCT CAG TCT G	RAS ATG GGG AGA GTG AAG CAG AA	1572bp IT
		RAS GTG AGT TTG CCA AGC AGT CA	2033bp WT
additional integration	Forward ATA ATA CCG CGC CAC ATA GC	RAS ATG GGG AGA GTG AAG CAG AA	1945bp
P1+P2	Forward CCA GCT CCC ATA GCT CAG TCT G	RAS GAA AAG GGA ACC CAG CGA GT	521bp
P1+P4	Forward CCA GCT CCC ATA GCT CAG TCT G	RAS ATG GGG AGA GTG AAG CAG AA	1569bp
P3+P4	Forward CTT GTA GGC CTG CAT CAT CA	RAS ATG GGG AGA GTG AAG CAG AA	963bp
P5+P7	Forward CAA CGT GCT GGT TAT TGT GC	RAS CAC CTT GAA GCG CAT GAA CT	1386bp
P6+P9	Forward GAG GAG AAT CCC GGC CCT AGG ATG GTG AGC AAG GGC GAG GAG G	RAS TTG AAT CTG TGA AGA CGG GC	773bp
P8+P12	Forward CAC CAT CGT GGA ACA GTA CG	RAS TGA AGA GCA GAG CCA GGA AC	1693bp
P10+P11	Forward CATG AAG CCC CTT GAG CATC	RAS CAG CTC AGG TTC TGG GAG AG	824bp
P1+P4+P13	Forward CCA GCT CCC ATA GCT CAG TCT G	RAS ATG GGG AGA GTG AAG CAG AA	1569bp WT
		RAS GTG AGT TTG CCA AGC AGT CA	2033bp IT

Table S2: Antibodies used for immunocytochemistry / flow cytometry

	Antibody	**Dilution**	**Company Cat# and RRID**
Pluripotency Markers	Mouse anti-OCT3/4	1:100	Santa Cruz Cat# sc-5279
	Mouse anti-TRA-1-60	1:100	Abcam Cat# 16288
	Mouse anti-SSEA4	1:100	DSHB Cat# MC813-70 (ab16287)
Differentiation Markers	Mouse anti-α-Fetoporotein	1:300	R&D Cat# MAB1368
	Mouse anti-α-Actinin, Sarcomeric	1:800	Sigma Aldrich Cat# A7811
	Mouse anti-β-3-Tubulin	1:400	Millipore Cat #05-559
Detection of human cells	Mouse anti-human-Nucleoli	1:400	Abcam Cat# ab190710
Secondary antibodies	Cy5 Donkey anti-mouse IgG	1:200	Jackson ImmunoResearch Labs Cat# 715-175-150,
	AF488 Donkey anti-goat IgG	1:200	Jackson ImmunoResearch Labs Cat# 705-545-147

Table S3: Overview of the Guide RNAs used for the Cas-mediated PCR-free enrichment of the construct sequence for Nanopore sequencing, including the respective sequences, PAMs (Protospacer Adjacent Motifs), strand information and position in the construct.

Guide No.	Sequence	PAM	Strand	Position in the construct
2134	AGTTGGGCGCGGGATCCGTA	AGG	+	6578-6597
2136	ACAATCTTCTCGACCGACAC	AGG	-	12439-12458
55	TTTGAGGACCTTCGACCAGC	TGG	+	12632-12652
2139	AATCCTACCTAACGCACTCC	TGG	-	18076-18095

Figure S1

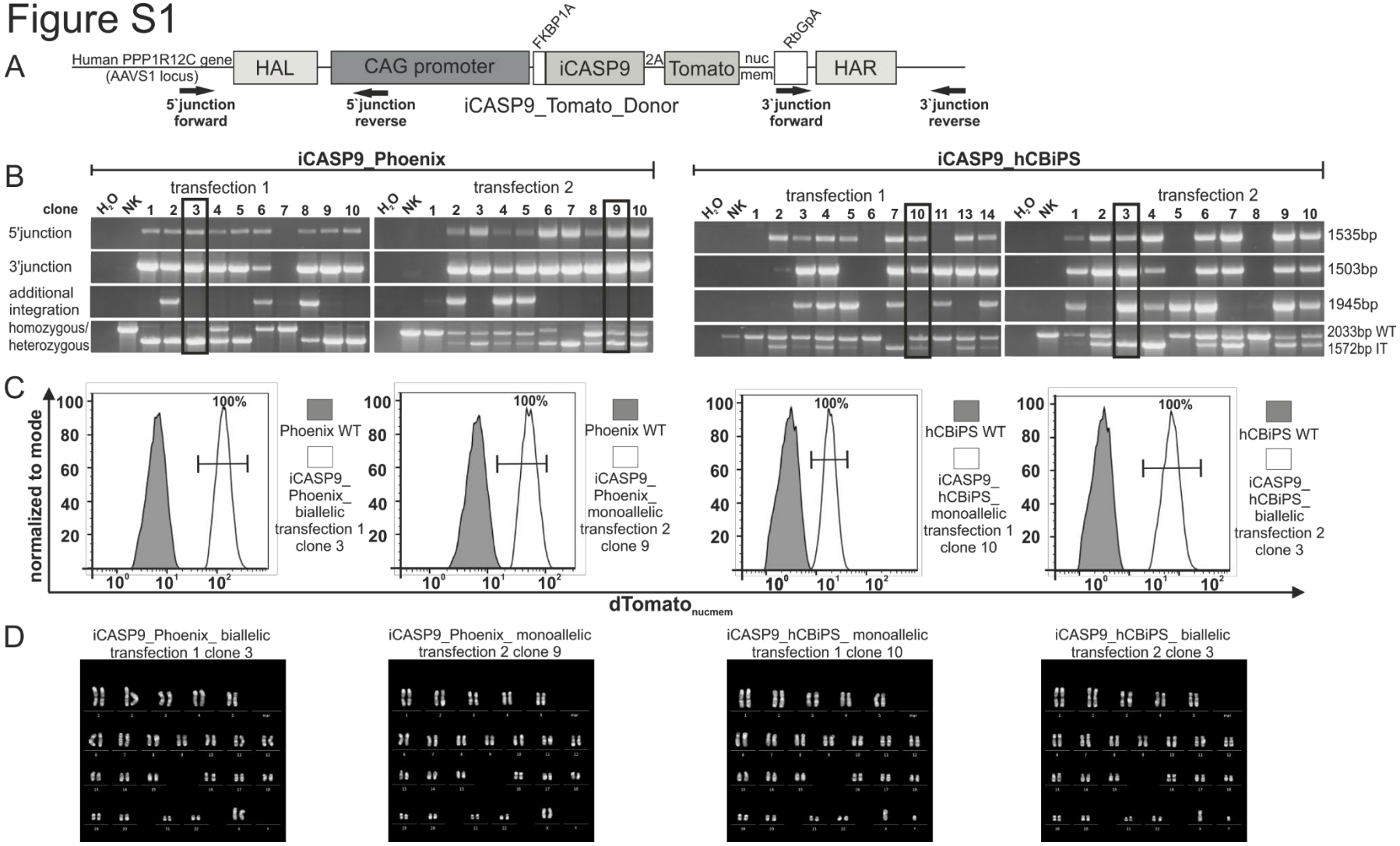
A
Human PPP1R12C gene
(AAVS1 locus)
HAL
CAG promoter
FKBP1A
iCASP9
2A
Tomato
nuc
mem
RbGpA
HAR
5`junction forward
5`junction reverse
iCASP9_Tomato_Donor
3`junction forward
3`junction reverse
B
iCASP9_Phoenix
iCASP9_hCBiPS
transfection 1
transfection 2
clone
H2O
NK
5'junction
3'junction
additional integration
homozygous/ heterozygous
1535bp
1503bp
1945bp
2033bp WT
1572bp IT
C
normalized to mode
100%
Phoenix WT
iCASP9_ Phoenix_ biallelic transfection 1 clone 3
iCASP9_ Phoenix_ monoallelic transfection 2 clone 9
hCBiPS WT
iCASP9_ hCBiPS_ monoallelic transfection 1 clone 10
iCASP9_ hCBiPS_ biallelic transfection 2 clone 3
dTomato nucmem
D
iCASP9_Phoenix_ biallelic transfection 1 clone 3
iCASP9_Phoenix_ monoallelic transfection 2 clone 9
iCASP9_hCBiPS_ monoallelic transfection 1 clone 10
iCASP9_hCBiPS_ biallelic transfection 2 clone 3

Figure S1: Four iCASP9 iPSC clones were selected for further studies based on genotyping and flow cytometric analysis of dTomato$_{nucmem}$ expression and karyotype analysis. A) Schematic illustration of primer combinations and locations used for genotyping of targeted iPSCs. B) Correctly targeted and dTomato$_{nucmem}^{pos}$ clones (marked with frames) were preselected based on demonstration of mono-/biallelic integration by junction PCRs on genomic DNA using primer pairs spanning the 5´- and the 3´- junction of the donor cassette and genomic AAVS1 sequence. Primers for additional integration are located in the backbone (AmpR, forward primer) and in the CAG promotor (reverse primer) of the donor backbone. Abbreviations: IT, integrated transgene; WT ,wild type. C) Expression of dTomato$_{nucmem}$ was analyzed via flow cytometry. Representative histograms for dTomato$_{nucmem}$ expression of transgenic clones are shown. D) Karyotype analysis demonstrated absence of larger genomic aberrations. Representative metaphases are shown. Chromosome analysis was performed following standard cytogenetic procedures. At least 15-20 metaphases per clone were analyzed.

Figure S2

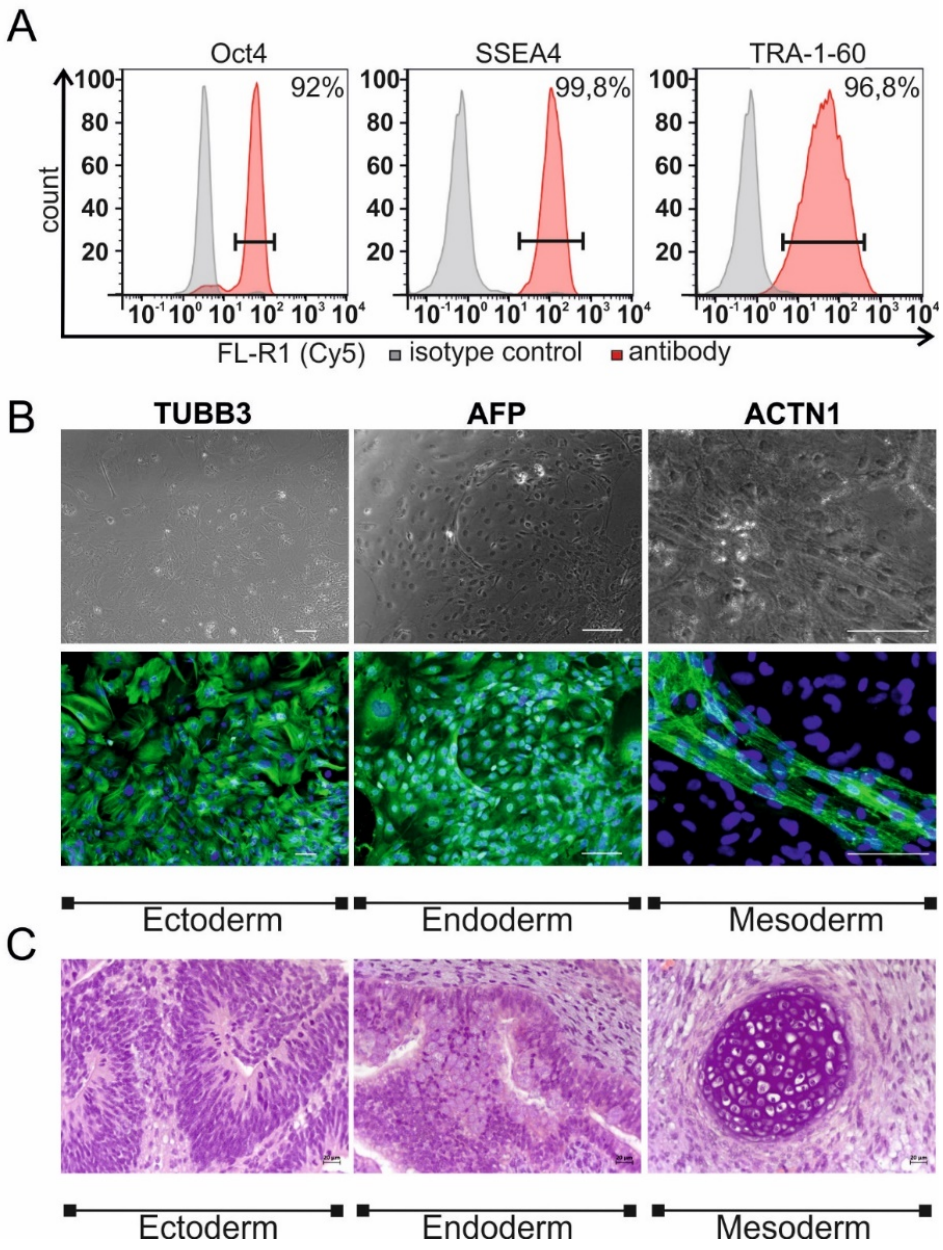

Figure S2: Characterization of iCASP9 hiPSCs (exemplarily shown for monoallelic iCASP Phoenix). A) Immunofluorescence staining of iCASP9 hiPSCs against OCT-3/4, SSEA4 and TRA-1-60 analyzed via flow cytometry demonstrate the expression of these typical pluripotency markers. B) Immunostaining of iCASP9 hiPSCs derivatives on d21 of differentiation revealed expression of ectodermal (TUBB3), endodermal (AFP), and mesodermal (ACTN1) marker proteins (green). Nuclei are stained with DAPI (blue). Scale bars: 100 µm. C) Injection of undifferentiated monoallelic iCASP9 Phoenix iPSCs into immunodeficient NOD*SCID* mice led to formation of teratomas containing derivatives of all three germ layers. Neural tube formation representing ectodermal differentiation. Endodermal epithelium with prominent mucus-producing cells representing endoderm and mesoderm formation. Chondrocytes showing mesoderm formation. (Scale bars represent 20 mm as depicted.)

Figure S3

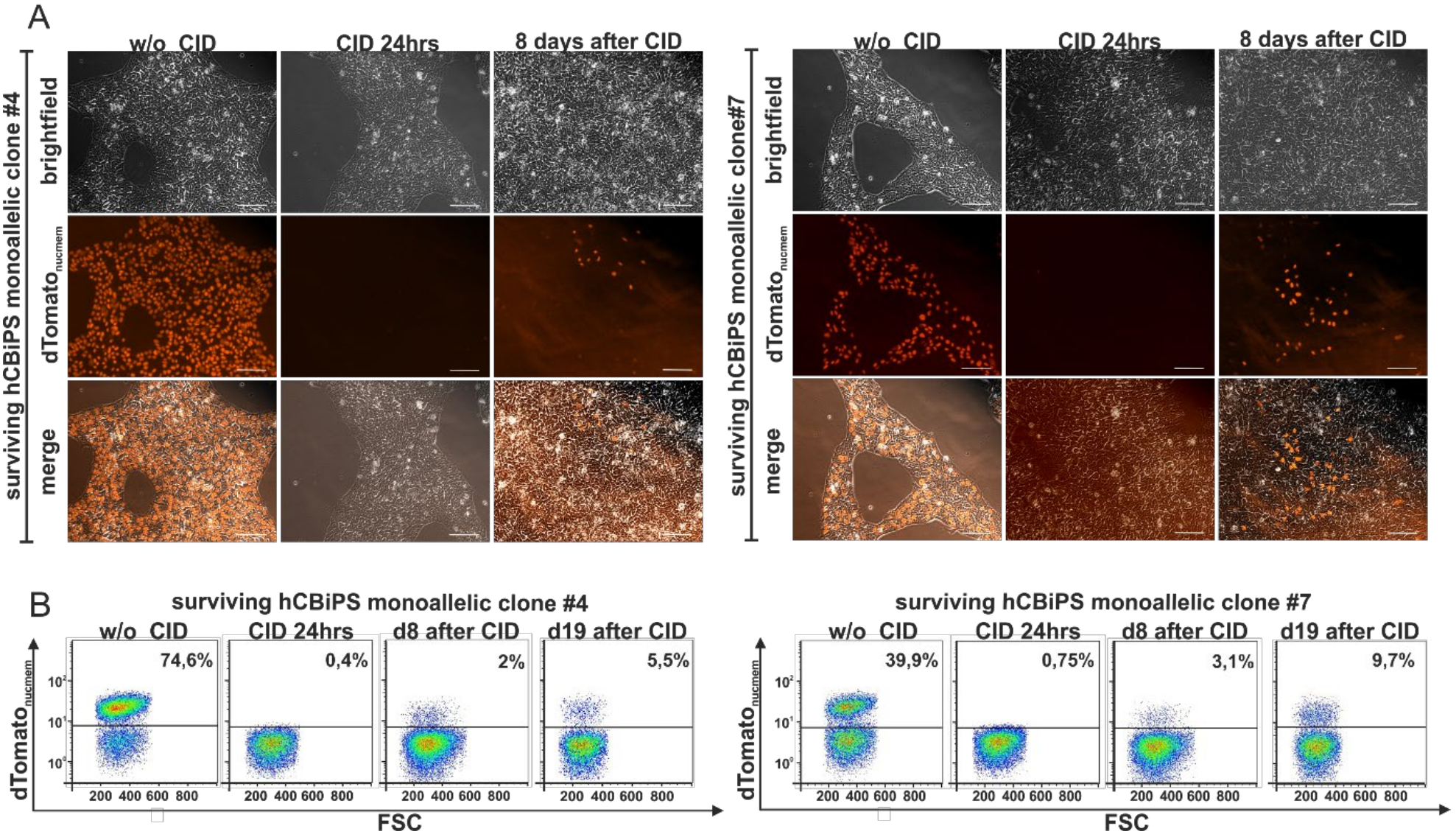
A
w/o CID
CID 24hrs
8 days after CID
surviving hCBiPS monoallelic clone #4
brightfield
dTomato nucmem
merge
surviving hCBiPS monoallelic clone#7
B
surviving hCBiPS monoallelic clone #4
w/o CID
CID 24hrs
d8 after CID
d19 after CID
74,6%
0,4%
2%
5,5%
dTomato nucmem
FSC
surviving hCBiPS monoallelic clone #7
39,9%
0,75%
3,1%
9,7%

Figure S3: dTomato$_{nucmem}^{neg}$ colonies that survived CID treatment partially regain dTomato$_{nucmem}$ expression after prolonged cultivation.

Representative microscopic images and flow cytometric analysis of two monoallelic iCASP9 hcBiPS2 subclones treated with CID are shown. Left panel: monoallelic iCASP9 subclone #4, right panel: monoallelic iCASP9 subclone #7.

A) Left columns: show monoallelic hCBiPS2 single cell clones that survived initial treatment with CID during recovery under feeder-based culture conditions. These cultures contain dTomato$_{nucmem}^{pos}$ and dTomato$_{nucmem}^{neg}$ cells (Stage iii in Figure 5A). Middle columns show the hCBiPS2 clones after 2nd CID treatment for 24 h applied to eliminate the dTomato$_{nucmem}^{pos}$ fraction. Surviving cells are dTomato$_{nucmem}^{neg}$ (Stage iv in Figure 5A). Right column: Starting eight days after CID-treatment increasing proportion of apparently non-methylated cells with detectable dTomato$_{nucmem}$ transgene expression could be observed (scale bar 100 µm).

B) Left columns: show monoallelic hCCBiPSC clones after a 2nd CID treatment for 24 hours to eliminate the dTomato$_{nucmem}^{pos}$ fraction. Surviving cells are dTomato$_{nucmem}^{neg}$ (Stage iv in Figure 5A). Middle right column: Starting eight days after CID-treatment new dTomato$_{nucmem}^{pos}$ cells could be observed (scale bar 100µm). Right column: 19 days after 2nd CID treatment the proportion of dTomato$_{nucmem}^{pos}$ cells had further increased suggesting continuous demethylation of the CAG promoter / PPP1R12C locus.

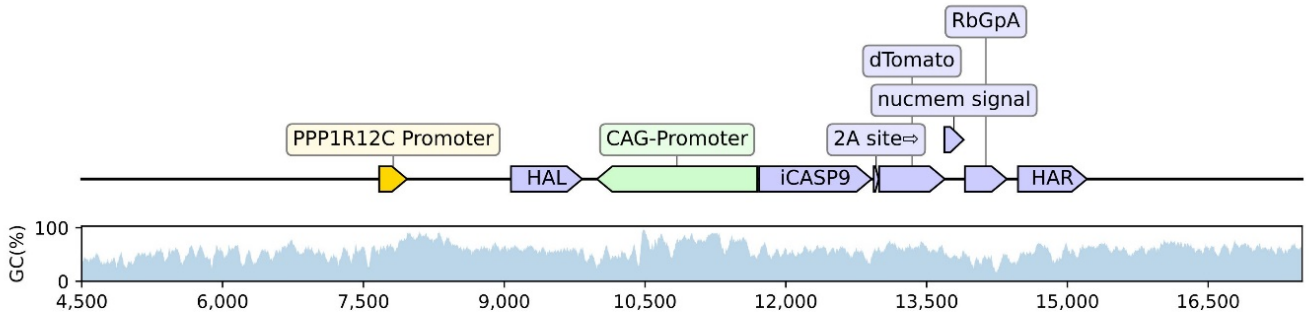

Figure S4: Schematic illustration of CpG contents in the iCASP9 suicide construct integrated into the AAVS1 locus. Content of CpGs is shown for the iCASP9 suicide construct and surrounding areas of the human PPP1R12C gene.

Figure S5

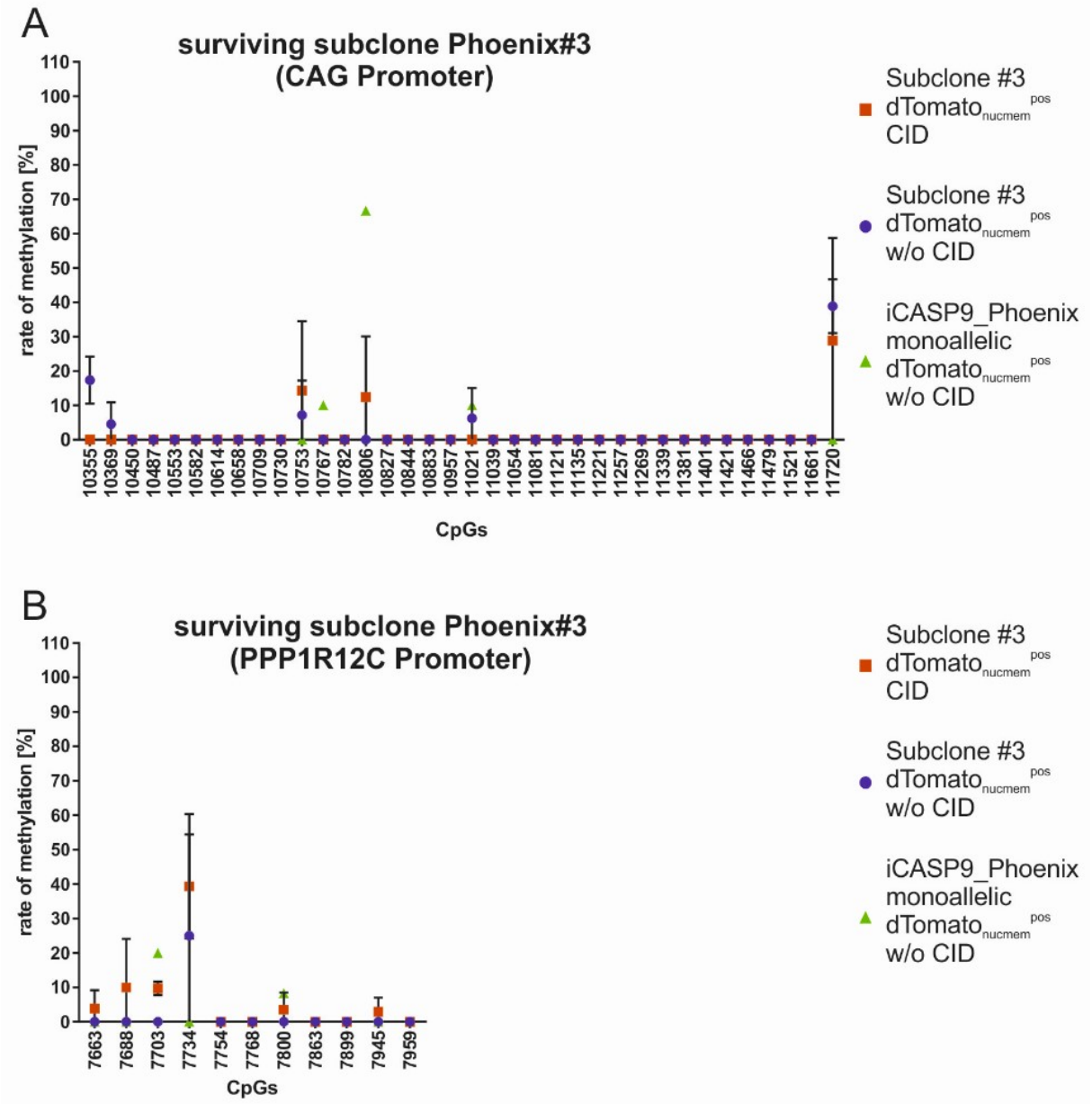

Figure S5: Nanopore Sequencing showed no elevated methylation of the CAG promoter and the endogenous PPP1R12C promoter in the CID resistant monoallelic Phoenix subclone #3. A) Analysis of CpGs in the CAG Promoter of surviving monoallelic subclone #3 did not provide evidence for increased methylation that could explain the survival of the CID treatment. B) In addition, the Nanopore Sequencing analysis of the PPP1R12C showed no changes in methylation status. Data are presented as mean ± SD (n = 2). A scheme of CpG islands in the AAVS1 locus and the integrated iCASP9 donor construct is shown in Figure S4.

Figure S6

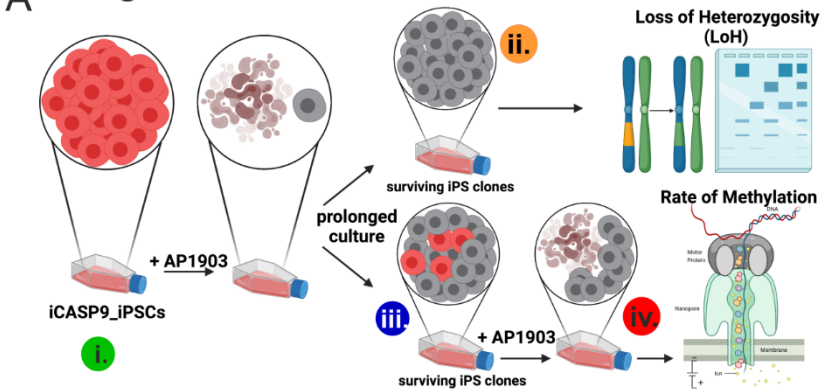
A
iCASP9_iPSCs
i.
+ AP1903
surviving iPS clones
ii.
prolonged culture
iii.
+ AP1903
surviving iPS clones
iv.
Loss of Heterozygosity (LoH)
Rate of Methylation

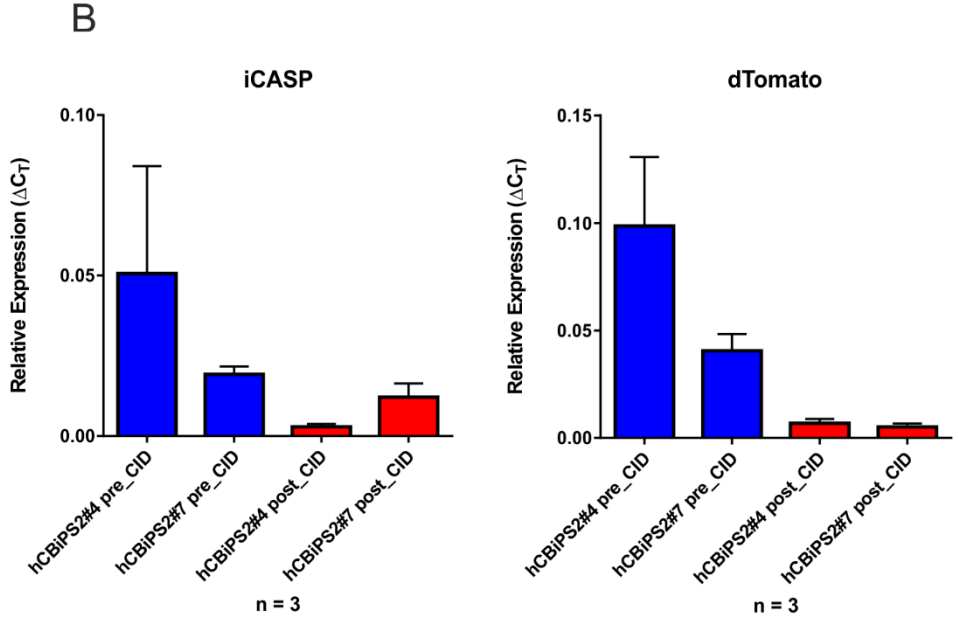
B
iCASP
Relative Expression (ΔCT)
0.10
0.05
0.00
hCBiPS2#4 pre_CID
hCBiPS2#7 pre_CID
hCBiPS2#4 post_CID
hCBiPS2#7 post_CID
n = 3
dTomato
Relative Expression (ΔCT)
0.15
0.10
0.05
0.00
hCBiPS2#4 pre_CID
hCBiPS2#7 pre_CID
hCBiPS2#4 post_CID
hCBiPS2#7 post_CID
n = 3

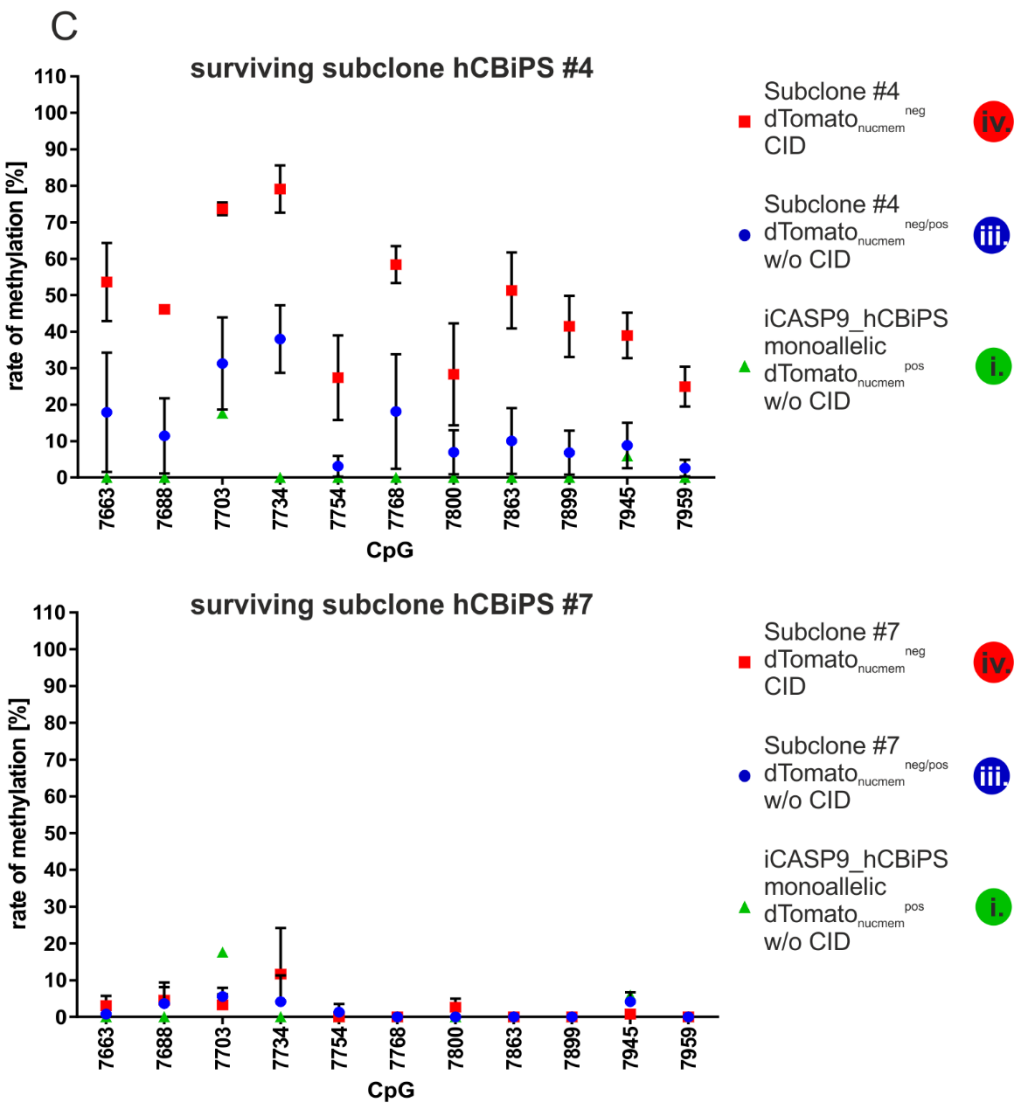
C
surviving subclone hCBiPS #4
rate of methylation [%]
110
100
90
80
70
60
50
40
30
20
10
0
7663
7688
7703
7734
7754
7768
7800
7863
7899
7945
7959
CpG
Subclone #4 dTomato nucmem neg CID
iv.
Subclone #4 dTomato nucmem neg/pos w/o CID
iii.
iCASP9_hCBiPS monoallelic dTomato nucmem pos w/o CID
i.
surviving subclone hCBiPS #7
rate of methylation [%]
CpG
Subclone #7 dTomato nucmem neg CID
iv.
Subclone #7 dTomato nucmem neg/pos w/o CID
iii.
iCASP9_hCBiPS monoallelic dTomato nucmem pos w/o CID
i.

Figure S6: Methylation of the endogenous PPP1R12C promoter may contribute to transgene silencing in CID resistant monoallelic iPSC subclones. A) Scheme illustrating appearance and selection for Tomato$_{nucmem}^{neg}$ cells resistant to CID-induced apoptosis and re-appearance of Tomato$_{nucmem}^{pos}$ CID-sensitive cells during culture expansion, and analysis of different stages for LoH and methylation of promoter elements (and surrounding genomic DNA, data not shown). Colored circles mark stages that have been further analyzed for promoter methylation.

B) Methylation of the CAG and the PPP1R12C promoter led to strong downregulation of the iCASP9 and Tomato$_{nucmem}^{neg}$ transgenes in hCBiPS2 subclones #4 and #7.

C) Nanopore Sequencing showed elevated methylation of the PPP1R12C promoter in one out of two analyzed CID-resistant monoallelic dTomato$_{nucmem}^{neg}$ hCBiPS2 subclones that both show methylation of the CAG promoter but did not show transgene elimination.